# Dynamic Analysis for Lunar Alightment

A. P. CAPPELLI*
*North American Aviation Inc., Downey, Calif.*

**One of the important problems to be encountered in a lunar exploratory mission is the successful landing (touchdown) of a space vehicle on the surface of the moon. A description of vehicle response during landing will allow the prediction of the success of a lunar alightment. This paper presents an analytical procedure that describes the landing dynamics of a lunar alightment vehicle. The motion of an impacting vehicle is defined by the classical Eulerian equations of rigid body motion. These equations were integrated numerically by the digital computer to obtain particular solutions. Landing stability curves for a typical lunar vehicle were derived from the particular results obtained with this analytical procedure. An idealized model representing a typical lunar vehicle is used in making the analysis. This model incorporates the use of three crushable landing legs to accomplish the dissipation of kinetic energy at impact. This paper includes a discussion of the alightment concept and the effects of lunar surface characteristics. The results of vehicle drop tests conducted at the Space and Information Systems Division of North American Aviation Inc. also are reported.**

## Nomenclature

$F_{cr}$ = force required to crush inelastic energy absorbing material, lb
$F_L$ = force required to crush lateral energy absorber, lb
$F_v$ = force required to crush vertical energy absorber, lb
$n$ = number of crushable landing legs
$X,Y,Z$ = fixed-in-body reference frame (Fig. 4)
$X',Y',Z'$ = fixed-in-space reference frame (Fig. 4)
$V_x,V_y,V_z$ = velocity components at the center of gravity of the vehicle referred to a frame of reference fixed in the body, fps
$\omega_x,\omega_y,\omega_z$ = angular velocity components about fixed body axes, rad/sec
$F_x,F_y,F_z$ = external force components acting on the vehicle in respective $X,Y,Z$ directions
$M_x,M_y,M_z$ = external moments acting on the vehicle about respective $X,Y,Z$ axes, ft-lb
$g_L$ = acceleration due to lunar gravity, ft/sec$^2$
$I_x,I_y,I_z$ = mass moments of inertia of the rigid body referred to coordinate axes fixed in the body, slug-ft$^2$
$m$ = mass of the vehicle, slugs
$\Delta t$ = time increment used in numerical integration, sec
$\Delta(\ )$ = change in $(\ )$
$V_{x1},V_{y1},V_{z1}$ = velocity components of leg tip 1 referred to body axes, fps
$V_{x2},V_{y2},V_{z2}$ = velocity components of leg tip 2 referred to body axes, fps
$V_{x3},V_{y3},V_{z3}$ = velocity components of leg tip 3 referred to body axes, fps
$V_x',V_y',V_z'$ = velocity components at center of gravity referred to a fixed space frame of reference, fps
$\dot{V}_x',\dot{V}_y',\dot{V}_z'$ = acceleration components at center of gravity referred to a fixed space frame of reference, ft/sec$^2$
$i$ = subscript indicating time interval, $i$ = 1,2,3, etc.
$\bar{X}',\bar{Y}',\bar{Z}'$ = vehicle coordinates at center of gravity referred to fixed space system, ft
$\Theta,\Phi,\Psi$ = Eulerian angles, deg; see Ref. 1 for definitions and sign conventions
$A$ = maximum slope inclination, deg (Fig. 4)
$B$ = orientation of maximum slope (projection) with respect to the fixed reference frame, deg (Fig. 4)
$\beta$ = lateral velocity direction, deg (Fig. 4)
$V_L$ = lateral touchdown velocity of vehicle, fps (Fig. 4)
$V_v$ = vertical touchdown velocity of vehicle, fps (Fig. 4)
$R_1,R_2,R_3,\ DCG$ = vehicle dimensions, ft (Fig. 4)
$\Delta D_1$ = amount of vertical crushing of leg 1, ft
$Z_1$ = vertical coordinate (referred to space frame) of leg tip 1, ft
$Z_{s1}$ = vertical coordinate of lunar slope corresponding to leg tip 1, ft
$V_0$ = vertical velocity of design analogy vehicle, fps
$d$ = stroke or depth of required crushable material, ft
$a$ = allowable vehicle deceleration, ft/sec$^2$
$\sigma_{cr}$ = crushing strength of energy absorption material, psi
$A_0$ = effective cross-sectional area of crushable material, in.$^2$
$S$ = $1/(\cos\Phi\cos\Theta - \cos\Theta\sin\Phi\tan A\cos B + \tan A\sin B\sin\Theta)$
$A_1$ = $\cos\Phi\cos\Psi$
$A_2$ = $(\sin\Phi\sin\Theta\cos\Psi - \cos\Phi\sin\Psi)$
$A_3$ = $(\cos\Phi\sin\Theta\cos\Psi + \sin\Phi\sin\Psi)$
$B_1$ = $(\cos\Theta\sin\Psi)$
$B_2$ = $(\sin\Phi\sin\Theta\sin\Psi + \cos\Theta\cos\Psi)$
$B_3$ = $(\cos\Phi\sin\Theta\sin\Psi - \sin\Phi\cos\Psi)$
$C_1$ = $-\sin\Theta$
$C_2$ = $\sin\Phi\cos\Theta$
$C_3$ = $\cos\Phi\cos\Theta$

Received by ARS August 20, 1962; revision received March 19, 1963. This paper is based on the results of an investigation that was conducted as part of a Space and Information Systems Division sponsored research program in Structural Sciences. The author acknowledges the valuable assistance of his colleague, W. D. Brayton, who assisted in the formulation of the solution and the preparation of the IBM program, and his colleagues in the Space and Information Systems Division Engineering Development Laboratory, who conducted the drop tests. The author also is indebted to Leonard A. Harris, who read the entire manuscript and offered many valuable suggestions.

* Senior Research Engineer, Applied Sciences, Space and Information Systems Division.

## I. Introduction

MAN is today on the threshold of an era of lunar exploration. One of the important problems to be encountered in a lunar exploratory mission is the successful touchdown of a vehicle on the surface of the moon. The ideal procedure in designing the lunar soft-landing would be to develop systems capabilities that would allow the spacecraft to search out a suitable landing site and to accomplish a gentle touchdown on the lunar surface. In reality, however, the space-

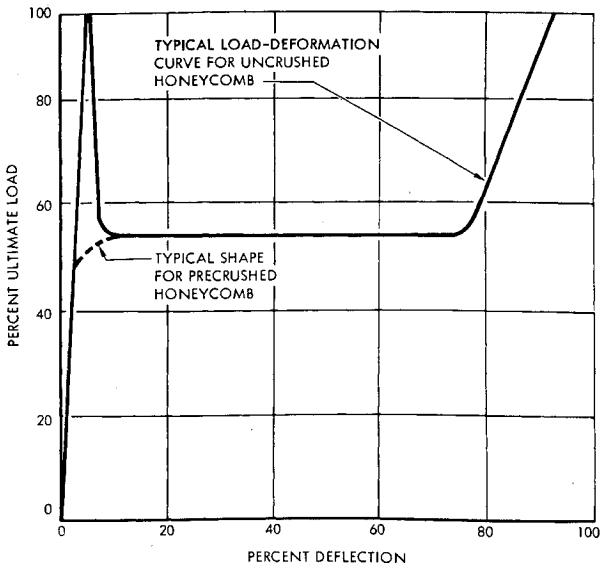


**Fig. 1 Force-displacement curve for honeycomb material**

craft systems are subject to a wide range of errors. A lunar alightment vehicle must be able to cope with the effects of inaccuracies expected from guidance, propulsion, sensing, and other systems. These inaccuracies may result in a multitude of landing conditions, which can include various vehicle approach velocities, vehicle orientations, and landing terrain characteristics.

For purposes of discussion, a summary of the requirements that will dictate a safe landing is presented in the following:

1) The vehicle must not overturn, i.e., it must remain stable during the alightment process. (This assumes, of course, that there is a desired final orientation, or state, of the vehicle.)

2) The impact forces and resulting accelerations must be reduced to tolerable limits to insure the integrity and performance of the vehicle payload (human or otherwise).

3) The vehicle rebound must be kept to a minimum.

4) The final position of the spacecraft must allow operation of the payload components.

A safe lunar landing is defined as an alightment maneuver that has been performed successfully within the preceding requirements, although the total mission may not have been successful. Requirements 2 and 3 can be met by employing a suitable energy-absorbing landing device or landing system. A suitable vehicle design will satisfy clearance requirements. The determination of a safe lunar landing, therefore, resolves itself to the description of the landing stability or overturn resistance of a lunar alightment vehicle. A complete description of the vehicle motion during the alightment maneuver will allow the determination of vehicle landing stability.

The purpose of this paper is to present an analytical technique that will describe the motion of a lunar alightment vehicle. Particular solutions of the motion equations are obtained by employing numerical techniques; the digital computer is used as the computational tool.

## II. Alightment Concept

The requirements of landing an instrumented or inhabited package on the surface of the moon in an operable condition generally will necessitate the use of some type of shock- or energy-absorbing device. One of the promising energy-absorption systems for soft landings is an internal crushable structure that allows vehicle deceleration on impact by some type of inelastic energy-absorption device. The kinetic energy at impact can be dissipated without rebound by plastic deformation or destruction of an expendable portion of the structure.

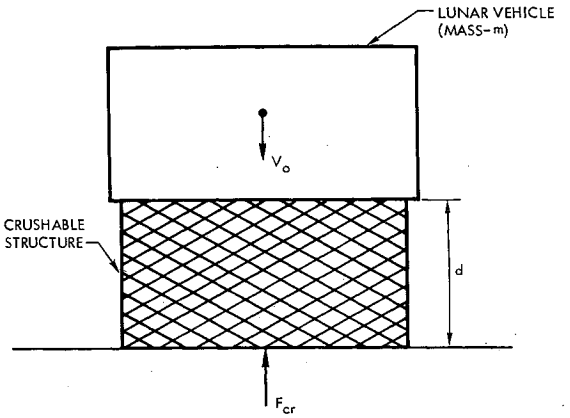


**Fig. 2 Lunar vehicle used for design analogy**

To bring the vehicle to rest, the kinetic energy at impact must be converted into strain energy of the deformed landing structure. The absorbed energy is equal to the area under the resisting force-displacement curve. Aluminum honeycomb core materials or balsa wood offer excellent energy-absorption characteristics for a crushable landing system.

An idealized compressive force-displacement diagram for precrushed aluminum honeycomb material is shown in Fig. 1. During the first application of load, honeycomb materials exhibit an initial peak load that is approximately two times as great as the subsequent flat-top deflection curve. Precrushing permanently removes the initial peak of the load deflection curve. A rectangular force-displacement curve occurs for approximately 75% of the total length of the honeycomb. The resulting rectangular pulse provides the unique advantage of a resisting function that offers constant external forces on the landing legs of the vehicle during impact. The allowable magnitude of vehicle deceleration is dictated by the design deceleration-load limitations on the payload and can be obtained by the selection of a crushable material that deforms plastically at a defined magnitude of crushing force $F_{cr}$. Very high deceleration onset rates, which may be intolerable for manned vehicles, are experienced with the use of a crushable landing system. This problem possibly could be alleviated by the proper contouring of the crushable structure.

## III. General Principles of Design for a Crushable Energy-Absorbing Structure

Before a dynamic analysis of an impacting lunar vehicle can be initiated, a complete description must be made of the vehicle landing system in order to determine the pertinent boundary conditions and to define the external forces. The techniques used in the design of a crushable landing system best can be shown by a simple example. Consider the vehicle shown in Fig. 2 with a touchdown vertical velocity of magnitude $V_0$ on impact with the lunar surface. The energy absorber for this case is a crushable block of material at the base of the vehicle. The kinetic energy of the vehicle at impact must be converted into strain energy of the deformed landing structure in order to bring the vehicle to rest. In equation form, the energy expression becomes

$$\tfrac{1}{2}mV_0^2 = F_{cr} \cdot d \tag{1}$$

where the strain energy of the crushable structure, the right side of Eq. (1), represents the area under the force-displacement curve shown in Fig. 1.

The allowable external force $F_{cr}$ required to crush the landing system is dictated by the deceleration limits placed on the payload. The magnitude of this force is determined from Newton's equation:

$$F_{cr} = ma \tag{2}$$

where $m$ is the vehicle mass, and $a$ represents the maximum deceleration that the vehicle is allowed to experience. A rectangular force-displacement curve assumes an infinite onset rate with the vehicle velocity reduced at a constant deceleration. The type and dimensions of the crushable material required to develop the crushing force $F_{cr}$ are determined by the expression

$$F_{cr} = \sigma_{cr} \cdot A_0 \tag{3}$$

where $\sigma_{cr}$ is the crushing strength of the material, and $A_0$ is the effective cross-sectional area. The depth or stroke $d$ of crushable material required to dissipate the kinetic energy is determined from Eq. (1). Thus, given a vehicle mass $m$, vertical impact velocity $V_0$, and allowable vehicle deceleration $a$, the design of the crushable structure landing gear can be completed. The preliminary design of a lateral energy absorber could be accomplished by employing a similar technique. Figure 3 shows a feasible design of an aluminum honeycomb crushable landing gear. This design uses a simple piston approach with provisions made for energy absorption in the vertical and lateral directions.

## IV. Lunar Surface Characteristics

Because the nature of the lunar surface is subject to speculation at this time, some assumptions have been made to support the landing dynamic analysis. Some of the lunar surface characteristics of major concern are bearing strength, surface inclination, coefficient of friction, and surface irregularities. In this study, the impacted lunar surface has been considered to be a rigid plane. Because a rigid surface allows for high deceleration, the activation of the energy absorbers and the dissipation of the kinetic energy are initiated at impact.

An assumption was made in the analysis that the coefficient of friction is considered to be sufficiently high, for all landing conditions, to develop the external forces required to crush the energy-absorbing materials. Because the crushing forces are known, the external forces acting on the impacting vehicle can be defined. These forces are considered to act on a landing leg when the leg is touching the lunar surface and the leg trip has a resultant velocity of motion. The energy absorbers used in the physical models contain lateral and vertical energy absorption characteristics. The magnitude of the slope on which a vehicle alights obviously will have an effect on the landing stability. Provisions have been made in the analysis for variations of this quantity in order to determine any significant effects.

## V. Analytical Procedure

The dynamic analysis of a lunar soft-landing spacecraft is achieved by considering the vehicle as a rigid body with the motion defined by the classical Eulerian equations of rigid body motion. An idealized model of a typical lunar vehicle upon which the dynamic analysis will be made is illustrated in Fig. 4. This model, which has an equilateral triangle planform, incorporates the use of three crushable landing legs to accomplish the dissipation of the kinetic energy at impact. In this study, the lateral energy absorbers are assumed to be located at the leg tips, rather than at the locations shown in the illustration. To simplify the analysis, the frame of reference adopted for the equations of motion is fixed in the vehicle and will be allowed to move with it. The coordinate axes are chosen coincident with the principal axes of the system, and the origin is located at the vehicle's center of gravity.

Because the frame of reference $(X,Y,Z)$ moves with the vehicle, the absolute position and orientation of the vehicle cannot be described relative to it. For this purpose, a fixed-in-space reference frame $(X',Y',Z')$ is introduced. The motion of the body referred to the moving frame of reference can be related to the fixed reference frame by means of the transformation equations, which will be introduced subsequently. In the preceding reference manner, it becomes possible to relate the absolute position of the center of gravity of the lunar vehicle to a chosen fixed datum (usually the lunar surface or a gravity direction). Because the vehicle is considered to be a rigid body, the motion of any point on the vehicle can be described in terms of the motion of the center of gravity. The simultaneous solution of the differential equations required to define the motion of the vehicle presents a formidable task; an appeal has been made to numerical integration techniques through use of the digital computer to obtain particular solutions.

In the development of the digital computer program, a description of the initial and boundary conditions is required before the solution of the equations can be accomplished. The initial conditions include the following: 1) the vehicle description, 2) the properties of the crushable landing system, 3) the inclination of the lunar surface, 4) the orientation of the vehicle at impact with respect to the lunar surface, 5) the vertical and lateral touchdown velocities of the vehicle, and 6) the angular velocity of the vehicle at impact.

The following equations, presented in finite difference form, represent the Eulerian equations of motion referred to the

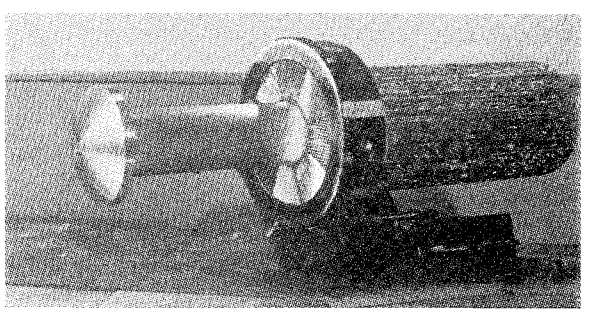

**Fig. 3 Crushable piston landing leg (vertical and lateral energy absorption)**

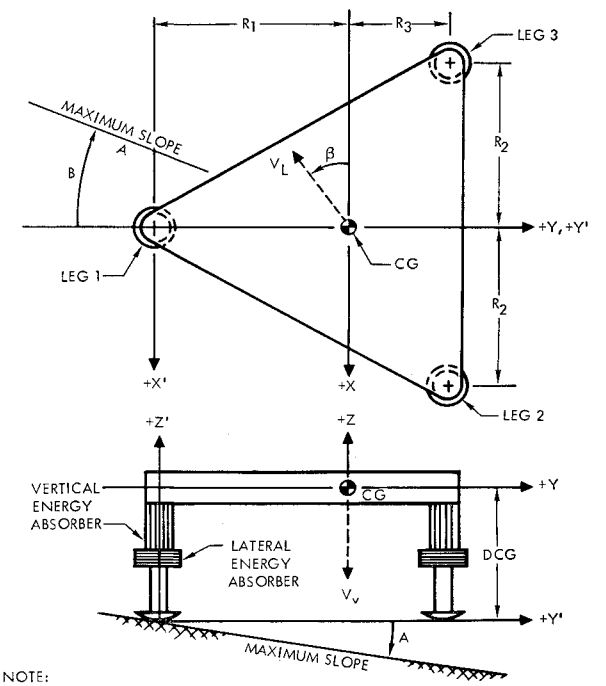


NOTE:

X,Y,Z DENOTES VEHICLE COORDINATE SYSTEM (ORIGIN AT C G)
X',Y',Z' DENOTES FIXED-IN-SPACE COORDINATE SYSTEM (ORIGIN AT THE INTERSECTION OF THE LUNAR SURFACE AND THE TIP OF LEG 1)

**Fig. 4 Lunar alightment vehicle**

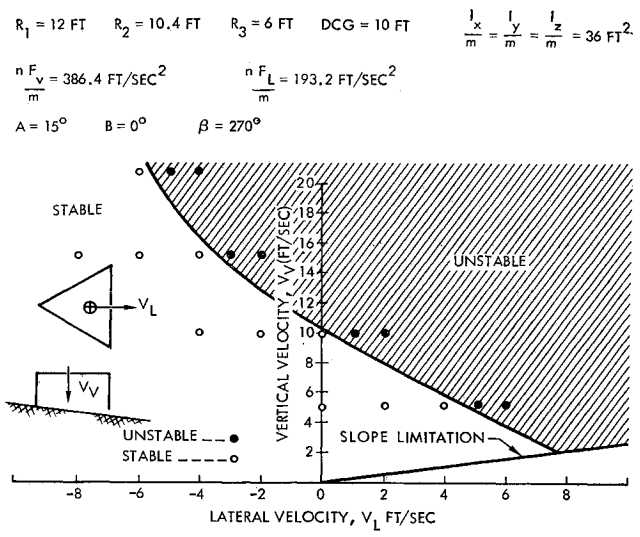


**Fig. 5 Landing stability of vehicle impacting a 15° slope initially on one leg (lateral velocity in direction of maximum slope)**

vehicle body axes (see Fig. 4):

$$\Delta V_x = [(F_x/m) - g_L \sin\Theta + V_y\omega_z - V_z\omega_y]\Delta t \quad (4)$$

$$\Delta V_y = [(F_y/m) + g_L \cos\Theta \sin\Phi + V_z\omega_x - V_x\omega_z]\Delta t \quad (5)$$

$$\Delta V_z = [(F_z/m) + g_L \cos\Theta \cos\Phi + V_x\omega_y - V_y\omega_x]\Delta t \quad (6)$$

$$\Delta\omega_x = \{(M_x/I_x) + \omega_z\omega_y[(I_y - I_z)/I_x]\}\Delta t \quad (7)$$

$$\Delta\omega_y = \{(M_y/I_y) + \omega_z\omega_x[(I_z - I_x)/I_y]\}\Delta t \quad (8)$$

$$\Delta\omega_z = \{(M_z/I_z) + \omega_x\omega_y[(I_x - I_y)/I_z]\}\Delta t \quad (9)$$

The preceding equations represent the change in the translational and rotational velocities at the vehicle center of gravity during an increment of time $\Delta t$ under the influence of the applied external forces ($F_x$, $F_y$, $F_z$, $M_x$, $M_y$, $M_z$).

The applications of external forces will manifest themselves in the dynamic analysis as boundary conditions. A definition of the time history of force applications will make possible the solution of the equations of motion. As stated previously, the force system acting on the alightment vehicle during impact can be defined when the properties of the crushable landing legs are described. The magnitude of the external forces will, in general, be dictated by the crushing strength of the honeycomb or of any other frangible material used in the landing system. These forces will be applied when a moving leg tip comes in contact with the lunar surface. The direction of the forces will be opposite to the direction of the velocity components at the leg tips. In reality, the legs will crush on impact with the rigid surface because the kinetic energy of the vehicle is considered to be dissipated by the application of the impact forces through some distance or stroke. The stroke represents the permanent deformation of the landing leg.

In preserving the rigid body analogy, the alightment vehicle theoretically will penetrate the lunar surface because of this stroke requirement. The distance (measured along the leg) that the fictitious uncrushed leg tip has penetrated the lunar surface represents the amount of vertical crushing of the energy absorber. This distance can be determined from the following equation:

$$\Delta D_1 = (Z_{s1} - Z_1)S \quad (10)$$

This expression represents penetration of leg 1 as shown in Fig. 4. Similar expressions can be written for the other landing legs. $Z_1$ is the vertical coordinate (referred to the fixed axes) of leg tip 1 at a specific time interval. The vertical coordinate of the lunar surface corresponding to this leg tip location is defined by $Z_{s1}$; $S$ is a function of the vehicle orientation, slope orientation, and slope inclination relating the vertical penetration distance to the distance measured along the landing leg. A positive value of $\Delta D_1$ indicates surface penetration. As long as the computed value of $\Delta D_1$ is greater than any previously computed value, the landing leg is considered to be in contact with the surface. The maximum positive value of $\Delta D_1$ represents the amount of permanent deformation of the vertical energy absorbers. When this function decreases in magnitude, the leg has lifted off the surface, and the external forces will be removed. Knowing the uncrushed (rigid body) leg tip locations, the crushed (actual) leg tip locations can be computed by subtracting the permanent deformation from the original leg length. The determination of the actual leg tip location will make it possible to determine whether or not the leg is in contact with the impacted surface. The external forces will be applied at locations on the rigid body model corresponding to the locations of the crushed landing leg tips. Thus it can be seen that, by manipulation of the rigid body concept, it is possible to describe the motion of the deformable vehicle by the equations of rigid body motion.

The external forces ($F_x$, $F_y$, and $F_z$) are the sums of force components acting at the leg tips during any increment of time $\Delta t$. The moments of the forces applied at the leg tips about the center of gravity are represented by $M_x$, $M_y$, and $M_z$ in Eqs. (7–9). After the computation of the change of velocities from Eqs. (4–9), the new resulting velocities after the time increment $\Delta t$ can be obtained from the following equations:

$$V_{xi+1} = V_{xi} + \Delta V_x \quad (11)$$

$$V_{yi+1} = V_{yi} + \Delta V_y \quad (12)$$

$$V_{zi+1} = V_{zi} + \Delta V_z \quad (13)$$

$$\omega_{xi+1} = \omega_{xi} + \Delta\omega_x \quad (14)$$

$$\omega_{yi+1} = \omega_{yi} + \Delta\omega_y \quad (15)$$

$$\omega_{zi+1} = \omega_{zi} + \Delta\omega_z \quad (16)$$

To establish the boundary conditions, it becomes necessary to describe the motion of each uncrushed leg tip. The velocities at the tip of an uncrushed leg can be described in terms of the center of gravity velocities and the angular velocities by the following expressions:

Leg 1

$$V_{x1} = V_x + (\omega_z \cdot R_1) - (\omega_y \cdot DCG) \quad (17)$$

$$V_{y1} = V_y + (\omega_x \cdot DCG) \quad (18)$$

$$V_{z1} = V_z - (\omega_x \cdot R_1) \quad (19)$$

Leg 2

$$V_{x2} = V_x - (\omega_z \cdot R_3) - (\omega_y \cdot DCG) \quad (20)$$

$$V_{y2} = V_y + (\omega_z \cdot R_2) + (\omega_x \cdot DCG) \quad (21)$$

$$V_{z2} = V_z + (\omega_x \cdot R_2) - (\omega_y \cdot R_2) \quad (22)$$

Leg 3

$$V_{x3} = V_x - (\omega_z \cdot R_3) - (\omega_y \cdot DCG) \quad (23)$$

$$V_{y3} = V_y - (\omega_z \cdot R_2) + (\omega_x \cdot DCG) \quad (24)$$

$$V_{z3} = V_z + (\omega_x \cdot R_3) + (\omega_y \cdot R_2) \quad (25)$$

The velocities at the crushed leg tip locations can be determined by substituting the crushed leg lengths for $DCG$ in the preceding expressions. These lengths will be the value of $DCG$ minus the permanent deformation of each leg determined from Eq. (10). The accelerations of each leg tip can be found in a similar manner.

The preceding motions refer to the vehicle body axes. The following equations transform the translatory velocities to a

fixed-in-space frame of reference:

$$V_x' = A_1V_x + A_2V_y + A_3V_z \quad (26)$$

$$V_y' = B_1V_x + B_3V_y + B_3V_z \quad (27)$$

$$V_z' = C_1V_x + C_2V_y + C_3V_z \quad (28)$$

The coefficients $A$, $B$, and $C$ are functions of the Eulerian angles $\Theta$, $\Phi$, and $\Psi$, which orient the body coordinate axes to the fixed space system. For sign conventions and definitions of the Eulerian angles, see Ref. 1. The change in the Eulerian angles $\Delta\Theta$, $\Delta\Phi$, and $\Delta\Psi$ during some time increment $\Delta t$ are

$$\Delta\Theta = (\omega_y \cos\Phi - \omega_z \sin\Phi)\Delta t \quad (29)$$

$$\Delta\Phi = (\omega_x + \omega_y \sin\Phi \tan\Theta + \omega_z \cos\Phi \tan\Theta)\Delta t \quad (30)$$

$$\Delta\Psi = (\omega_y \sin\Phi \sec\Theta + \omega_z \cos\Phi \sec\Theta)\Delta t \quad (31)$$

The new values of the Eulerian angles then are obtained from the following relationships:

$$\Theta_{i+1} = \Theta_i + \Delta\Theta \quad (32)$$

$$\Phi_{i+1} = \Phi_i + \Delta\Phi \quad (33)$$

$$\Psi_{i+1} = \Psi_i + \Delta\Psi \quad (34)$$

The new position of the center of gravity of the rigid body relative to the fixed-in-space frame of reference after a time interval $\Delta t$ can be represented by the following series expansions if the acceleration is assumed constant during the time interval:

$$\bar{X}_{i+1}' = \bar{X}_i' + V_{xi}'\,\Delta t + \dot{V}_{xi}'[(\Delta t)^2/2] \quad (35)$$

$$\bar{Y}_{i+1}' = \bar{Y}_i' + V_{yi}'\,\Delta t + \dot{V}_{yi}'[(\Delta t)^2/2] \quad (36)$$

$$\bar{Z}_{i+1}' = \bar{Z}_i' + V_{zi}'\,\Delta t + \dot{V}_{zi}'[(\Delta t)^2/2] \quad (37)$$

The position of each leg tip or of any point on the rigid body can be described in a similar manner.

The determination of the new position of the leg tips will allow the description of the boundary conditions for the next time interval. With the new position and orientation of the vehicle and the new boundary conditions that result, iteration of the analytical procedure restarting with Eq. (4) will describe a new vehicle position for the next time interval.

The change in geometry of the lunar vehicle caused by crushing of the lateral energy absorber has been neglected in the analysis because of the small geometrical changes encountered and the resulting small changes in the external moment due to shortening of the moment lever arms. However, the magnitude of the lateral reaction is included and may influence the landing stability of the vehicle. This integration process can be repeated until the vehicle has stopped motion or has reached an unstable condition of overturning. These limitations can be stipulated in the computer program through the use of conditional statements. Thus, through the outlined integration process, the absolute motion of the impacting vehicle can be defined. The computer program can be modified easily to treat many different vehicle configurations and landing systems.

## VI. Failure Criteria for Overturn

The landing system must insure the stability of the lunar alightment vehicle, during and after impact, for all limiting magnitudes of vertical and lateral touchdown velocities. The limiting magnitudes of these velocities are established by the guidance and propulsion systems. The dynamic analysis will indicate whether the impacting vehicle will remain stable within the terminal velocity limitations. The design of the energy absorbers also will be dictated by these velocities. The allowable magnitudes of the vertical and lateral terminal velocities can be plotted to obtain a critical

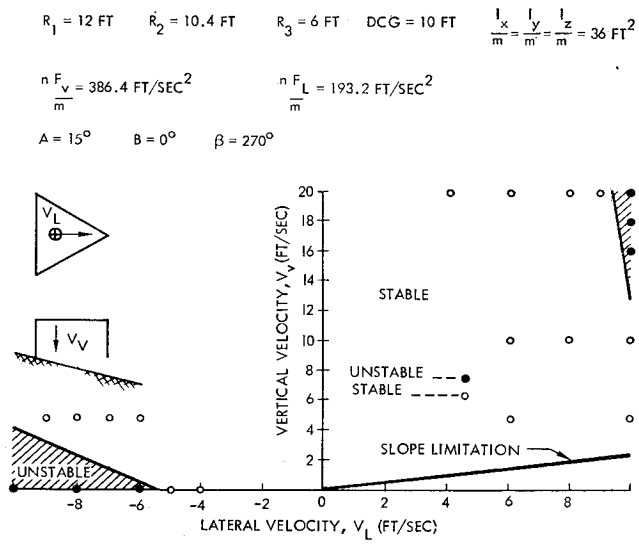


**Fig. 6 Landing stability of vehicle impacting a 15° slope initially on two legs (lateral velocity in direction of maximum slope)**

overturn envelope for a particular landing system. This envelope of the vertical vs lateral velocity combinations will indicate whether or not the design limitations have been satisfied.

The overturn criterion manifests itself in the computer program in the form of conditional statements. When the angular orientation of the vehicle exceeds specific values of the Eulerian angles, the vehicle is considered unstable. The Eulerian angles of concern are the angles $\phi$ and $\theta$. The critical magnitudes of these angles are dictated by the vehicle geometry and the angle of the impacted lunar slope. The critical values are established essentially at orientations where the vehicle would be statically unstable. In essence, the center of gravity must be located to produce a righting rather than an overturning moment on the vehicle during alightment. The impacted surface has been assumed to be a plane surface; effects of small surface irregularities that could be expected on the lunar surface have been neglected.

## VII. Results of the Analysis

Several test cases[2] were run to illustrate the results obtained from the digital computer program. Figures 5–7 represent the landing stability curves of the vehicle shown in Fig. 4 impacting a 15° inclined surface. The specific vehicle

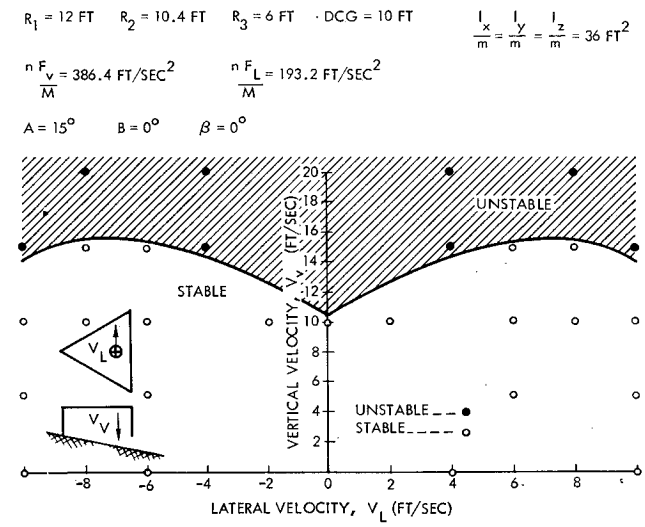


**Fig. 7 Landing stability of vehicle impacting a 15° slope initially on one leg (lateral velocity directed perpendicular to maximum slope)**

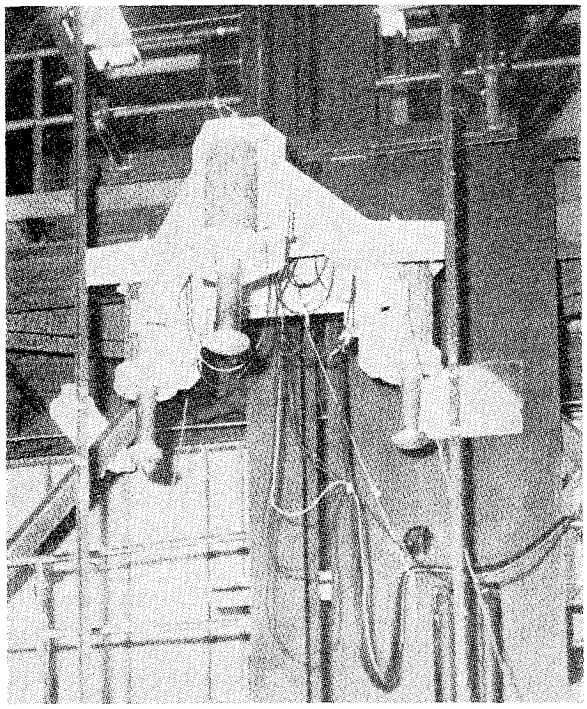

Fig. 8 Test vehicle prior to drop

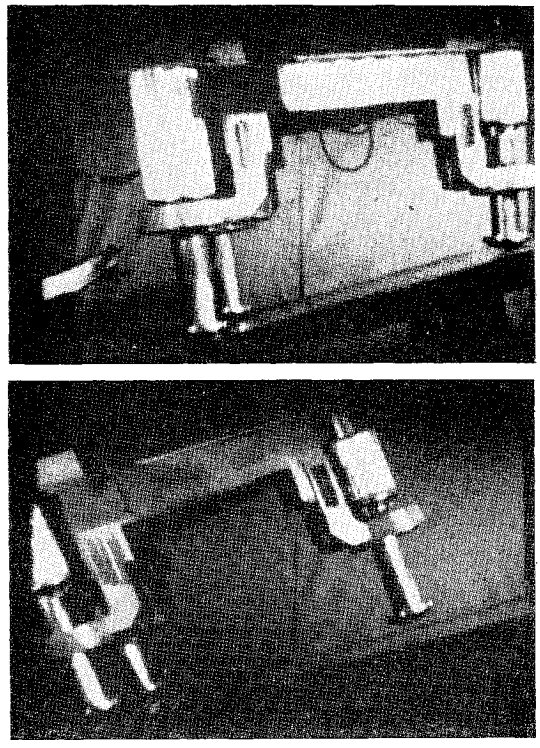


Fig. 9 Sequence photographs of 29.3-fps drop impact on 15° surface, one leg uphill (unstable)

geometries are described in the illustrations; each curve represents the landing stability for the illustrated landing conditions. The instability regions (shaded portions) indicate the vertical and lateral touchdown velocity combinations at which the vehicle will overturn during the alightment maneuver. It will be the function of the spacecraft's systems to maintain velocities in the described stable regions to prevent the vehicle from overturning upon touchdown. For the case of a landing on a slope, there will exist combinations of vertical and lateral velocities for which the vehicle will not impact the surface. This limitation due to the velocity and slope is designated by the slope limitation curves in Figs. 5 and 6. For velocity combinations below the slope limitation line, the vehicle will not impact the surface, and stability cannot be determined unless a change in slope or velocity is encountered.

In Fig. 5, the vehicle is considered to impact symmetrically the slope initially on one leg with the lateral velocity directed along the slope. This landing condition appears to be the most critical of the three landing conditions. A realistic velocity control envelope for this landing condition would dictate a maximum vertical velocity of 6 fps and an allowable lateral velocity in the limits $\pm 3$ fps. For the other landing conditions (shown in Figs. 6 and 7), the velocity envelopes could be maintained at considerably higher levels. The use of a finite difference technique requires the maintenance of small increments of time $\Delta t$ to obtain a reasonable degree of accuracy in the results. For the results presented, a time increment of 0.001 sec was considered satisfactory.

In addition to determining landing stability, the output of the program also indicates the final vehicle position and the amount of crushing of the vertical and lateral energy absorbers. It should be reiterated that the basic program can be modified to accommodate many different vehicles and landing systems.

## VIII. Discussion of Results

The results presented in Figs. 5–7 indicate the stability of a lunar vehicle for the landing conditions considered. It was the purpose of these curves to illustrate the type of results obtained from the analytical procedure developed in this paper. Because all landing conditions were not investigated, it is not possible to evaluate precisely the probability of success for the vehicle considered. In the future design of a lunar vehicle, it would be desirable to determine the landing safety for all critical landing conditions. For preliminary design purposes, it also would be helpful to determine the effect of vehicle configuration on landing stability. Because the analytical procedure can accommodate many vehicle configurations and landing conditions, the possibilities for the development of parametric trade-offs become numerous.

## IX. Drop Test Results and Conclusions

A series of vehicle drop tests were conducted by the Space and Information Systems Division Laboratory to verify a landing system design for the proposed Surveyor vehicle. Four vehicle drops were performed: two were performed on a flat surface, and two on a 15° sloping surface. The vertical impact velocity for the tests was approximately 29.3 fps. The first two drops were designed to test the vertical energy absorbers of the landing system. Figure 8 illustrates the test setup for the vehicle drops. For the third drop on the 15° surface, the vehicle was orientated with zero attitude so that two legs would impact the surface simultaneously and the third leg would impact down the slope slightly later. The analysis indicated that this drop would be stable, and these data were borne out by the test. The final position of the vehicle was slightly farther downslope than predicted by the analysis because the high frictional resistance expected in the analysis could not be attained in the test. The slight rebound of the inclined plane also may have contributed to the final position of the model.

The vehicle orientation was reversed for the fourth drop, which was on the 15° slope. For this drop, one leg impacted uphill, and the other two legs simultaneously hit downslope slightly later. The analysis indicated that the vehicle would be unstable for this orientation. The high-speed motion pictures of the test substantiated the analysis. Figure 9 shows the sequence clips from the films of this drop. After the last sequence photograph, the vehicle began to rotate about the two downhill legs and consequently overturned.

## References

[1] Etkin, B., *Dynamics of Flight* (John Wiley and Sons Inc., New York, 1959), p. 100.

[2] Goldstone, N. J., "Landing shock absorption," North American Aviation, Space and Information Systems Div., MD60-389 (December 1960); also 1961 Proceedings of the Institute of Environmental Sciences (1961).


MAY 1963 AIAA JOURNAL VOL. 1, NO. 5

# A Variational Launch Window Study

W. E. Miner* and Robert Silber†

*NASA George C. Marshall Space Flight Center, Huntsville, Ala.*

**In this paper the problem of establishing a circular orbit in a prespecified space-fixed plane is considered with the viewpoint of establishing performance penalties resulting from deviations in launch time from optimum launch time. The purpose is to obtain, as a function of allowable performance loss, a launch window, i.e., a certain time interval about the optimum launch time within which launch may occur, resulting in no more than the allowable performance loss. The analysis is performed using a three-dimensional calculus of variations flight deck for flight out of the atmosphere, resulting in optimum maneuvers both in and out of plane. Hence, the performance figure that results is strictly a function of the launch time. The orbital plane of basic interest is that of minimum inclination obtainable by a two-dimensional injection from Cape Canaveral. Variations of a few degrees below this value are considered to determine the minimal expense for plane changes.**

## Introduction

THE investigations that are discussed herein were made for a defined vehicle, a Saturn V. It is desired to launch this vehicle from Cape Canaveral into a circular orbit that lies in a specified plane. For this study, the altitude and the plane of the orbit are parameterized, i.e., more than one set of conditions are considered.

Any particular plane for the orbit can be considered as being defined by its inclination to the equatorial plane, for if one considers two planes of the same inclination, any trajectories establishing an orbit in one of the planes will do exactly the same in the other if launch occurs at an appropriately different time of day. The specified plane therefore is definable by a single parameter.

For a reference plane, that inclination for which a circular orbit can be established with the least propellant expenditure is taken. Such a plane would have very nearly the inclination equal in magnitude to the latitude of the launch site, for it would be established with the use of a due-east launch azimuth in order to obtain maximum benefit from the rotation of the earth. But because of the rotation of the earth, it will not be exactly the plane of inclination of the launch site, and the segment of trajectory through the atmosphere will not lie exactly in a plane.

However, these differences are slight in comparison to the variations to be considered. Therefore, bearing in mind that the reference plane actually differs by a slight amount in inclination from the latitude of the launch site, the authors nevertheless will refer to the reference plane as that plane with inclination equal in magnitude to the latitude of the launch site. Furthermore, it will be considered that the trajectory leading to injection into the circular orbit in this plane lies entirely within this plane if launch occurs at precisely that instant of the day when the launch site passes through the reference plane.

Other planes for the circular orbit will be defined by the parameter $\Delta i$, which is the difference in inclination from that of the reference plane; $\Delta i$ is positive for inclinations greater than that of the reference plane.

If the altitude of the circular orbit is denoted by $h$, it is clear that the desired orbit is specified by the two parameters $\Delta i$ and $h$. For this reason, these two parameters will be referred to as the *orbit parameters*. The values of $\Delta i$ considered are generally less than 2° in magnitude. The values of $h$ considered are 100 km, 100 naut miles, 150 naut miles, and 200 naut miles.

Assume now that a particular set of orbit parameters has been selected. One then faces the problem of determining the best time of day for launch. For example, for the reference plane ($\Delta i = 0$), the best time of day for launch is that instant of the day when the launch site passes through the reference plane, resulting in a two-dimensional trajectory. Variations from this launch time will result in a deterioriation of performance, i.e., in an increase in propellant expenditure. Generally, one can expect that, for each value of $\Delta i$ under consideration, it is possible to establish a certain best, or optimum, launch time.

Furthermore, it is not reasonable to assume that the launch azimuth is unimportant. Indeed, one of the major results of this study is the demonstration of a significant dependence of performance on launch azimuth. It will be seen that, for each set of orbit parameters, a certain optimum launch azimuth corresponds to each time of launch. Thus, the establishment of the launch window entails the determination of the expense of variations of launch time from the optimum launch time, and, for the final analysis, to each nonoptimum launch time should be associated the optimum launch azimuth for that launch time.

## Launch Parameters

It has been seen that both the launch time and the launch azimuth are available for optimization, and the major part of this investigation consists of establishing optimum trajectories

Presented at the ARS 17th Annual Meeting and Space Flight Exposition, Los Angeles, Calif., November 13–18, 1962; revision received March 11, 1963.

* Deputy Chief, Future Projects Branch, Aeroballistics Division. Member AIAA.

† Aerospace Engineer, Future Projects Branch, Aeroballistics Division.